Frascati Physics Series Vol. 76 (2024)
8th young researchers' workshop 'Physics Challenges in the LHC Era'
May 13 and 16, 2024

Kaonic atoms studies with SIDDHARTA-2 at DAΦNE

Kairo Toho
Research Center for Accelerator and Radioisotope Science (RARiS), Tohoku University, Japan

L. Abbene[1], F. Artibani[1,14], M. Bazzi[1], G. Borghi[4,5], M. Bragadireanu[7], A. Buttacavoli[2], M. Cargnelli[3], M. Carminati[4,5], A. Clozza[1], F. Clozza[1], L. De Paolis[1], R. Del Grande[1,8], K. Dulski[1,11], C. Fiorini[4,5], I. Frišči[6], C. Guaraldo[1†], M. Iliescu[1], M. Iwasaki[9], A. Khreptak[10], S. Manti[1], J. Marton[3], P. Moskal[10,11], F. Napolitano[1], S. Niedzwiecki[10,11], H. Ohnishi[12], K. Piscicchia[13,1], F. Principato[2], A. Scordo[1], F. Sgaramella[1], M. Silarski[10], D. Sirghi[1,7,13], F. Sirghi[1,7], M. Shurzok[10,11], A. Spallone[1], L. Toscano[4,5] M. Tuechler[3], J. Zmeskal[3†] and Catalina Curceanu[1]

[1] Laboratori Nazionali di Frascati, INFN, Via E. Fermi 54, 00044 Frascati, Italy
[2] Dipartimento di Fisica e Chimica - Emilio Segrè, Università di Palermo, Viale Delle Scienze, Edificio 18, Palermo, 90128, Italy
[3] Stefan-Meyer-Institut für ubatomare Physik, Dominikanerbastei 16, Wien, 1010, Austria
[4] Politecnico di Milano - Dipartimento di Elettronica, Informazione e Bioingegneria, Via Giuseppe Ponzio 34, Milano, 20133, Italy
[5] INFN Sezione di Milano, Via Giovanni Celoria 16, Milano, 20133, Italy
[6] Department of Physics, Faculty of Science, University of Zagreb, Bijenička cesta 32, Zagreb, 10000, Croatia
[7] Horia Hulubei National Institute of Physics and Nuclear Engineering (IFIN-HH), No. 30, Reactorului Street, Magurele, Ilfov, 077125, Romania
[8] Physik Department E62, Technische Universität München, James-Franck-Straße 1, Garching, 85748, Germany
[9] Institute of Physical and Chemical Research, RIKEN, 2-1 Hirosawa, Wako, Saitama, 351-0198, Japan
[10] Faculty of Physics, Astronomy, and Applied Computer Science, Jagiellonian University, Łojasiewicza 11, Krakow, 30-348, Poland
[11] Centre for Theranostics, Jagiellonian University , Kopernika 40, Krakow, 31-501, Poland
[12] Research Center for Accelerator and Radioisotope Science (RARiS), Tohoku University, Japan
[13] Centro Ricerche Enrico Fermi - Museo Storico della Fisica e Centro Studi e Ricerche "Enrico Fermi", Via Panisperna 89A, Roma, 00184, Italy
[14] Università degli studi di Roma Tre, Dipartimento di Fisica, Roma, Italy
[†] Deceased

Abstract

The SIDDHARTA-2 experiment advances the study of kaonic atoms, focusing on kaonic deuterium and other kaonic atoms, such as neon, to explore low-energy Quantum Chromodynamics (QCD). Utilizing Silicon Drift Detectors and sophisticated veto systems, the experiment conducts high-precision X-ray spectroscopy to measure strong interaction-induced shifts and broadenings of atomic energy levels. This enables investigations of both electromagnetic and non-perturbative QCD effects, with high-n transitions facilitating precision tests of Quantum Electrodynamics (QED) and lower-level transitions providing insights into antikaon-nuclei strong interaction. Preliminary observations in kaonic neon highlight the potential for bridging theoretical predictions and experimental results.

1 Scientific case

The strong interaction, one of nature's four fundamental forces known so far, is crucial for understanding the structure and stability of matter. Governed by Quantum Chromodynamics (QCD), it explains quark-gluon interactions, which are the building blocks of protons, neutrons, and hadrons. Despite significant advances, the low-energy behavior of QCD remains poorly understood due to its non-perturbative nature, necessitating innovative experiments to provide data for refining theoretical models.

Kaonic atoms, which involve a negatively charged kaon bound to a nucleus via electromagnetic interaction, serve as a precise probe for low-energy QCD, particularly in the strangeness sector. These systems are significant for several reasons: they enable investigations of low-energy QCD in systems with non-zero strangeness quantum number, provide data to test QED predictions, and facilitate the determination of the charged kaon mass.

2 Kaonic atom formation

In kaonic atoms, a negatively charged kaon replaces one of the orbital electrons, allowing investigations into both the strong interaction and QED. A kaonic atom forms when a kaon, either slowed down or possessing sufficiently low initial momentum, is captured by an atom through electromagnetic interaction after being stopped in a target. This process leads to a highly excited state, with the excitation level dependent on the system's reduced mass; in kaonic hydrogen, this occurs at approximately n $\sim$ 25 [1].

High-n energy transitions in kaonic atoms are primarily governed by electromagnetic interactions, with the strong interaction playing a negligible role. This enables the study of purely quantum electrodynamic (QED) effects, addressing fundamental issues such as the charged kaon mass puzzle [2]. By precisely measuring X-ray emissions from these transitions, one can compare observed results with purely QED-calculated values. Following capture, the kaonic atom begins to de-excite towards its fundamental state, emitting radiation in the X-ray domain as shown in Figure 1. However, the de-excitation process is influenced by the Stark effect and other competing mechanisms, particularly in higher-density environments, which significantly impact the yield of kaons fully de-exciting to the ground state.

Conversely, lower-level transitions in kaonic atoms provide critical insights into the non-perturbative regime of QCD. These transitions reflect the complex interplay of the strong interaction between the kaon and the nucleus, inducing an energy shift in the transition to the fundamental 1s level that deviates from the canonical electromagnetic value, $E^{em}_{2p\rightarrow 1s}$. This reveals the isospin-dependent antikaon-nucleon scattering lengths, which are fundamental for understanding low-energy QCD in the strangeness sector [3]. Thus, kaonic atoms serve as an invaluable tool for advancing our understanding of both electromagnetic and hadronic physics, bridging the gap between QED and non-perturbative QCD.

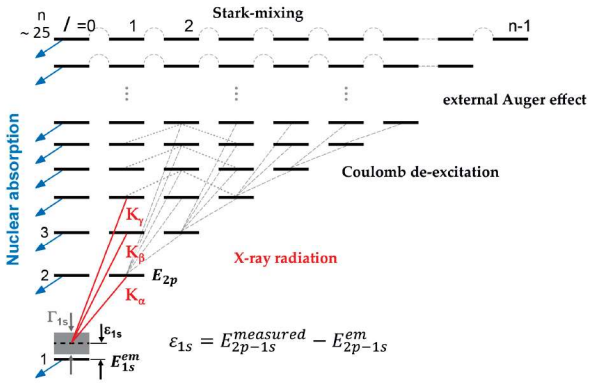

Figure 1: A schematic overview of the de-excitations which take place during the formation of the kaonic atoms. The kaons are captured in a highly excited state and cascade down to the fundamental level. The last transitions are influenced by the strong interaction, leading to a broadening and shift of the 1s level with respect to the case of only electromagnetic interaction. Reproduced from [4].

3 SIDDHARTA-2 Experiment

The SIDDHARTA-2 experiment aims to perform high-precision X-ray spectroscopy of kaonic atoms. Its primary goal is to measure the strong interaction-induced shift and width of the fundamental level in kaonic deuterium. Building on the earlier SIDDHARTA project on kaonic hydrogen, it exploits a new generation of Silicon Drift Detectors [5] [6] and three veto systems to tackle challenges of lower X-ray yield and wider 1s level width, or kaonic deuterium measurement.

The SIDDHARTA-2 setup is shown in Figure 2, installed above the DAΦNE interaction point in 2022. It was developed for high-precision spectroscopy in a high-radiation environment, handling both electromagnetic and hadronic background noise. Electromagnetic background from beam loss particles are reduced through time information from the Kaon Trigger and Silicon Drift Detectors (SDDs), while hadronic background is suppressed using sophisticated veto systems. The apparatus features a cylindrical beam pipe, a high-vacuum system, and a cryogenic target cell surrounded by 384 SDDs and multiple veto systems, with additional detection systems such as the Kaon Trigger [7] and Luminosity Monitor [8].

The Kaon Trigger, with plastic scintillators and Photomultiplier Tubes (PMTs), detects K^+K^- pairs and minimizes accidental triggers. The Luminosity Monitor assesses beam quality using similar scintillator technology. The cryogenic target cell, cooled to 20 K, and the SDDs, cooled to 140 K, optimize kaon stopping efficiency. The setup also includes Veto-1, an outer barrel of plastic scintillators, that reduces kaon backgrounds, while Veto-2 [9], composed of plastic scintillators tiles and Silicon Photomultipliers (SiPMs), addresses background from Minimum Ionising Particles (MIPs).

Calibration is done with two X-ray tubes (Jupiter 5000 Series, 50kV), installed on opposite sides of the vacuum chamber, and titanium-copper foils mounted on the target cell. The X-ray tubes excite fluorescence in these elements, producing characteristic Ti Kα and Cu Kα lines, which are used to calibrate the SDDs. The calibration peaks are fitted using Gaussian and tail functions to enhance accuracy, achieving a precision of 2.0 $\pm$ 0.1 eV when compared to the Fe Kα reference value, ensuring the stability required for kaonic deuterium measurements [10].

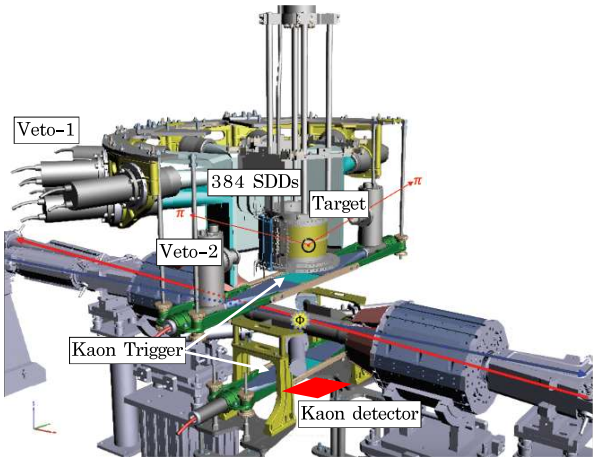

Figure 2: The schematic layout of the SIDDHARTA-2 experimental apparatus is presented, highlighting the main elements integral to the experiment.

4 Energy calibration of the Silicon Drift Detectors

The energy response function of an SDD detector for fluorescence X-ray signals is primarily characterized by a Gaussian function. However, a low-energy component exists due to incomplete charge collection and the electron-hole recombination effect. Consequently, the total peak fitting function is composed of two components:

- Gaussian function: This is the main contributor to the peak shape, with the peak width (σ) described by a function of the Fano Factor (FF), electron-hole pair creation energy (ε), and both electronic and thermal noise($noise$).
  The Gaussian function is expressed as:

$$G(E) = \frac{A_G}{\sqrt{2\pi}\sigma} \cdot e^{\frac{-(E-E_0)^2}{2\sigma^2}}, \sigma = \sqrt{FF \cdot \epsilon \cdot E + \frac{noise^2}{2.35^2}} \tag{1}$$

- Tail function: An exponential function accounts for incomplete charge collection, expressed as:

$$T(E) = \frac{A_T}{2\beta\sigma} \cdot e^{\frac{E-E_0}{\beta\sigma}+\frac{1}{2\beta^2}} \cdot erfc(\frac{E-E_0}{\sqrt{2}\sigma} + \frac{1}{\sqrt{2}\beta}) \tag{2}$$

In these equations, A_G and A_T represent the amplitudes of the Gaussian and tail functions, respectively. The parameter β is the slope of the tail, and erfc is the complementary error function. Figure 3 shows a typical energy spectrum obtained from a single SDD in a calibration run. For this analysis, the energy range was selected from 4 keV to 15 keV, encompassing the region of interest (ROI) for SIDDHARTA-2. For each target element, both the K_α and K_β transitions are clearly observed. The fitting function consists of a convolution of a Gaussian and a tail functions for each fluorescence line, while the background is modeled by a combination of a first-degree polynomial and an exponential function. The fitting process was conducted using MINUIT [12], with MIGRAD minimization yielding in this case a reduced chi-square value of 1.18, confirming the overall fit accuracy.

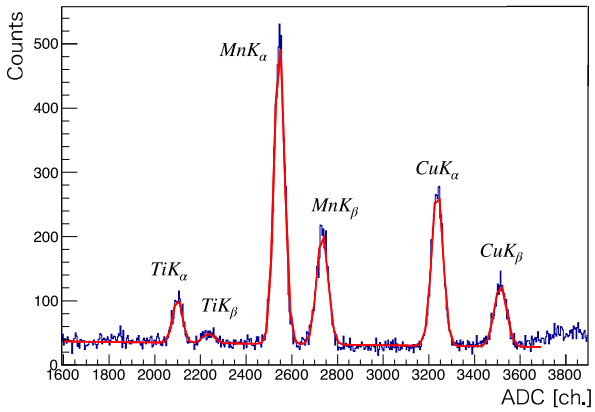

Figure 3: A typical Silicon Drift Detector energy spectrum acquired during a calibration run, in arbitrary ADC units, displays fluorescence emission lines from a multi-element target activated by an X-ray tube.

The K_α lines were selected to investigate the energy response of the SDDs due to their higher signal-to-noise ratio compared to the K_β lines. The energy response of the SDDs is described by a linear function based on the Analog-to-Digital Converter (ADC) response:

$$E = m \cdot ADC(ch.) + q \tag{3}$$

where m is the gain of the detector in eV/ch. Figure 4 illustrates the calibration function for the SDD spectrum in Figure 3. The calibration points are determined by the theoretical energy values of each line and their corresponding measured values in arbitrary ADC units.

The calibration accuracy and validity of the linearity assumption were assessed by calculating the residuals, defined as the difference between each calibrated point E_{meas} and its theoretical value E_{th} [13]:

$$\Delta E = E_{meas} - E_{th} \tag{4}$$

This analysis was applied to all 384 SDDs used in the SIDDHARTA-2 experiment. Figure 5 provides an example of the residuals plot for four SDDs. The residuals are centered around zero, with deviations of no more than 3 eV from the ideal linear case, indicating a linear response ($\Delta E/E$) with an accuracy better than 10^{-3}.

5 Kaonic neon observation: preliminary result

In the spring of 2023, prior to the kaonic deuterium measurement, a kaonic neon measurement was performed as part of the SIDDHARTA-2 optimization phase, with the objective of calibrating and refining the detectors' energy response. The target cell of the setup was filled with neon gas at a density equivalent to 0.36% of the liquid neon density (LNeD), and a total of 125 pb^{-1} of data was collected.

The calibration procedure previously described was applied to obtain the energy spectrum shown in Figure 6 corresponding to about 32 pb^{-1}. Five kaonic neon transitions were observed; these high-n transitions are not influenced by the strong kaon-nucleus interaction. Data analysis is ongoing towards a dedicated publication. This characteristic renders them particularly valuable for precision QED tests, as for determining the mass of charged kaons and exploring de-excitation mechanisms in kaonic atoms which are ongoing within the collaboration.

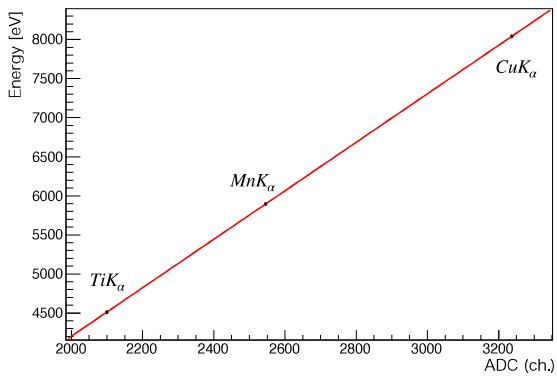

Figure 4: The linear calibration function translates ADC values to energy for the analyzed Silicon Drift Detector (SDD).

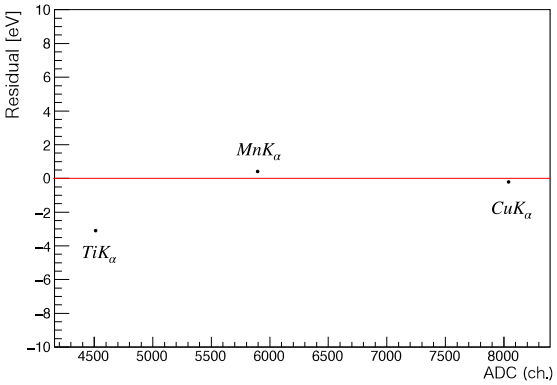

Figure 5: Residuals plot for a single SDD.

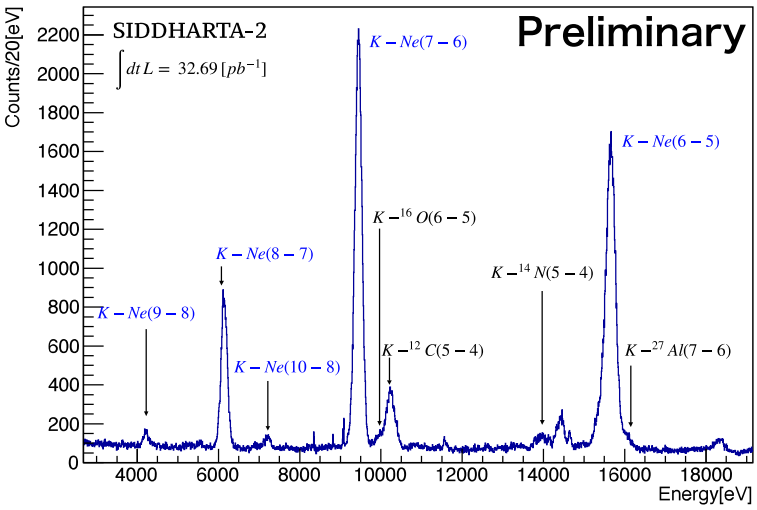

Figure 6: Preliminary kaonic neon energy spectrum, displaying lines for kaonic neon (K-Ne), carbon (K-C), nitrogen (K-N), oxygen (K-O), and aluminium (K-Al). Transitions are identified by the initial (n_i) and final (n_f) principal quantum numbers of the corresponding atomic levels.

6 Conclusions

The SIDDHARTA-2 experiment represents a significant advancement in the study of kaonic atoms, particularly in its efforts to probe the low-energy regime of Quantum Chromodynamics (QCD) and enhance our understanding of fundamental interactions.

The formation of kaonic atoms facilitates unique investigations into both electromagnetic and non-perturbative QCD effects. High-n energy transitions in kaonic systems serve as a platform for precision tests of Quantum Electrodynamics (QED), while lower-level transitions reveal vital information about the strong interaction and its influence on atomic energy levels.

The successful implementation of advanced detection systems, including Silicon Drift Detectors and sophisticated veto mechanisms, has significantly improved the accuracy and efficiency of measurements

in a challenging experimental environment. Preliminary observations, such as those in kaonic neon, underline the potential of these systems also for precision QED studies, thereby bridging the gap between theoretical predictions and experimental realities.

Through ongoing research and data analysis, the SIDDHARTA-2 collaboration aims to refine our understanding of the strong interaction and its manifestations in exotic atomic systems. This endeavor not only contributes to the fundamental physics landscape but also opens avenues for future explorations in hadronic physics.

7 Acknowledgements

We thank C. Capoccia from LNF-INFN and H. Schneider, L. Stohwasser, and D. Pristauz-Telsnigg from Stefan Meyer-Institut for their fundamental contribution in designing and building the SIDDHARTA-2 setup. We thank as well the DAΦNE staff for the excellent working conditions and permanent support. Part of this work was supported by the EU STRONG-2020 project (Grant Agreement No. 824093). The authors acknowledge support from the SciMat and qLife Priority Research Areas budget under the program Excellence Initiative—Research University at the Jagiellonian University.

References

1. F. Napolitano *et al.* Phys. Scr. 97 (2022) 084006
2. Bosnar D, Bazzi M, Cargnelli M, Clozza A, Curceanu C, Del Grande R, et al. Revisiting the charged kaon mass. Acta Phys Polon B (2020) 51:115. doi:10.5506/ aphyspolb.51.115
3. Curceanu C et al. 2020 Symmetry 12 ISSN 2073-8994
4. F Napolitano et al 2022 Phys. Scr. 97 084006
5. M. Bazzi *et al.* Condens. Matter 2021, 6(4), 47
6. F. Sgaramella *et al.* 2022 Phys. Scr. 97 114002
7. F. Sirghi *et al.* arXiv:2311.16144 [physics.ins-det]
8. M. Skurzok *et al.* 2020 JINST 15 P10010
9. M. Tüchler et al 2023 JINST 18 P11026
10. F. Sgaramella *et al.* Volume 59, article number 56, (2023)
11. Zyla, P. A. et al. Review of Particle Physics. PTEP 2020, 083C01 (2020).
12. James, F. MINUIT Function Minimization and Error Analysis: Reference Manual Version 94.1 (1994).
13. Vaughan, D. X-ray data booklet. center for x-ray optics. [tables] (1985). URL https://www.osti.gov/biblio/6359890.